CRYSTALLIZATION PAPERS

Acta Cryst. (1998). D**54**, 975–981

Crystallization of CcdB

MINH-HOA DAO-THI,[a] LODE WYNS,[a] FREDDY POORTMANS,[b] EL MUSTAFA BAHASSI,[c] MARTINE COUTURIER[c] AND REMY LORIS[a]* *at* [a]*Laboratorium voor Ultrastructuur, Vlaams Interuniversitair Instituut Biotechnologie, Vrije Universiteit Brussel, Paardenstraat 65, B-1640 Sint-Genesius-Rode, Belgium,* [b]*VITO, Boeretang 200, 2400 Mol, Belgium, and* [c]*Laboratoire de Génétique, Département de Biologie Moléculaire, Université Libre de Bruxelles, Paardenstraat 67, B-1640 Sint-Genesius-Rode, Belgium.*
E-mail: reloris@vub.ac.be

(*Received 3 July 1997; accepted 22 August 1997*)

Abstract

CcdB is a small dimeric protein that poisons DNA–topoisomerase II complexes. Its crystallization properties in terms of precipitant type, precipitant concentration, pH and protein concentration have been investigated leading to a novel crystal form which, in contrast to previously reported crystals, is suitable for structure determination using the multiple isomorphous replacement (MIR) method. The space group of this new form is $C2$, with unit-cell parameters $a = 74.94$, $b = 36.24$, $c = 35.77$ Å, $\beta = 115.27°$. The asymmetric unit contains a single monomer. Flash-frozen crystals diffract to at least 1.5 Å resolution, while room-temperature diffraction can be observed up to 1.6 Å. The double mutant S74C/G77Q, which acts as a super-killer, crystallizes in space group $I222$ (or $I2_12_12_1$) with unit-cell dimensions $a = 105.58$, $b = 105.80$, $c = 91.90$ Å. These crystals diffract to 2.5 Å resolution.

1. Introduction

The *Escherichia coli* F-plasmid is very stable when inherited in the bacterial population. Plasmid-carrying cells are able to propagate while daughter cells that have not inherited a plasmid copy are selectively killed (Jaffé *et al.*, 1985). The plasmid F-encoded proteins CcdA and CcdB are the key molecules responsible for this post-segregational killing of bacterial cells. The underlying mechanism is based on a differential decay of the activities of the CcdA and CcdB proteins (the half-life of the cytotoxic CcdB being longer than the half-life of CcdA) that antagonizes the CcdB action (Van Melderen *et al.*, 1994, 1996). When CcdA is absent, CcdB is responsible for cell death, induction of the SOS pathway and inhibition of DNA synthesis (Bex *et al.*, 1983; Karoui *et al.*, 1983; Bailone *et al.*, 1985). CcdA and CcdB are encoded by the *ccd* operon (Miki, Yashioka *et al.*, 1984; Miki, Chang *et al.*, 1984). They are known to auto-regulate their own expression and it was shown that both proteins act as a DNA binding repressor, probably after having formed a CcdA/CcdB complex (Tam & Kline, 1989*a*,*b*; De Feyter *et al.*, 1989). Recently, it was demonstrated that the CcdB-mediated cell killing involves poisoning of DNA–topoisomerase II complexes (Bernard & Couturier, 1992). The Arg462Cys mutation in the DNA gyrase A domain suppresses the lethal character of CcdB. Further experiments showed that, like quinolone antibiotics and a variety of anti-tumour drugs, CcdB is responsible for gyrase-mediated double-stranded DNA breakage (Bernard *et al.*, 1993). It thus converts the wide-type gyrase in a DNA-damaging agent. This action, which is most likely the result of direct binding of CcdB to the DNA gyrase A domain, can be completely reversed by addition of stochiometric amounts of CcdA.

Poisons of eucaryotic topoisomerases are regarded as potent candidates for anti-cancer drugs. Elucidation of the structure and mode of action of the CcdB protein may lead to the design of new antibiotics and anti-tumoural drugs. Efforts to crystallize CcdB over the last few years has led to the identification of experimental conditions for the growth of several crystal forms. Here we present information concerning the crystallization behaviour of CcdB and report on a novel crystal form that diffracts to high resolution and is suitable for structure determination. We also report the crystallization of a mutant that acts as a super killer, probably because of its enhanced affinity for the A subunits of gyrase.

2. Materials and methods

2.1. *Protein expression and purification of CcdB from E. coli*

CcdB was overexpressed in *E. coli* strain MS501 (containing the CcdB permissive mutation R462C in the *GyrA* gene-harbouring plasmid pULB2250). *E. coli* cells were grown at 310 K in LB medium supplemented with 100 mg l^{-1} ampicillin and streptomycin. When the optical density of the culture reached about 1.0 at 600 nm, expression of CcdB was induced by adding 0.5 m*M* IPTG. The culture was centrifuged and the resulting pellet stored overnight at 259 K. The pellet was resuspended in 50 m*M* Tris–HCl, 1 m*M* EDTA, 1 m*M* DTT, 150 m*M* NaCl and 10% glycerol (pH = 7.8). After sonication, cell debris was removed by centrifugation, and a 30–80% ammonium sulfate cut-off was applied. The ammonium sulfate pellet was redissolved in 50 m*M* Tris, 1 m*M* DTT (pH = 8.5) and applied to a QEAE column. Protein was eluted using a linear gradient of 0.0–1.0 *M* NaCl. Fractions containing CcdB were concentrated into a 5 ml volume and applied to a Superdex-75 gel-filtration column. Finally, the CcdB fractions were dialysed against 50 m*M* MOPS, 1 m*M* DTT (pH = 6.8) and applied to a Pharmacia Mono-S column. This column was again eluted with a 0.0–1.0 *M* NaCl gradient. This resulted in a protein showing only a single band on SDS–PAGE and a yield of about 20 mg CcdB per litre of culture. The purified protein was dialysed against water and concentrated to 15.0 mg ml^{-1} (assuming a specific absorption coefficient of 16 100 M^{-1} at 280 nm) and subsequently used in crystallization trials.

2.2. *Purification of the CcdB cysteine mutants*

The CcdB mutants S70C, S74C, S84C and the double mutant S74C/G77Q were purified by affinity chromatography on activated thio-Sepharose. After sonication of the cells, the cell debris was removed by centrifugation. The supernatant was applied to the affinity matrix in batch at 277 K and left overnight. Then the affinity column was packed and washed manually with a buffer containing 50 m*M* Tris–HCl (pH 7.80), 1 m*M* EDTA, 0.5 *M* NaCl and 0.1% Triton X-100. Triton X-100 was subsequently removed by a further wash with the same buffer, but with 20 m*M* DTT substituted for Triton X-100. The fractions containing CcdB were pooled and dialysed against a 50 m*M* Tris–HCl buffer, pH 8.5, loaded to a Mono-Q column and finally eluted from this column using a 0.0–1.0 *M* NaCl gradient. The pure protein was dialysed against water and concentrated before use in crystallization trials.

2.3. *Crystallization*

Crystallization conditions were screened using the hanging-drop method and resulted in three crystal forms, the details of which are summarized in Table 1. Phase diagrams were also determined by crystallization using the hanging-drop method.

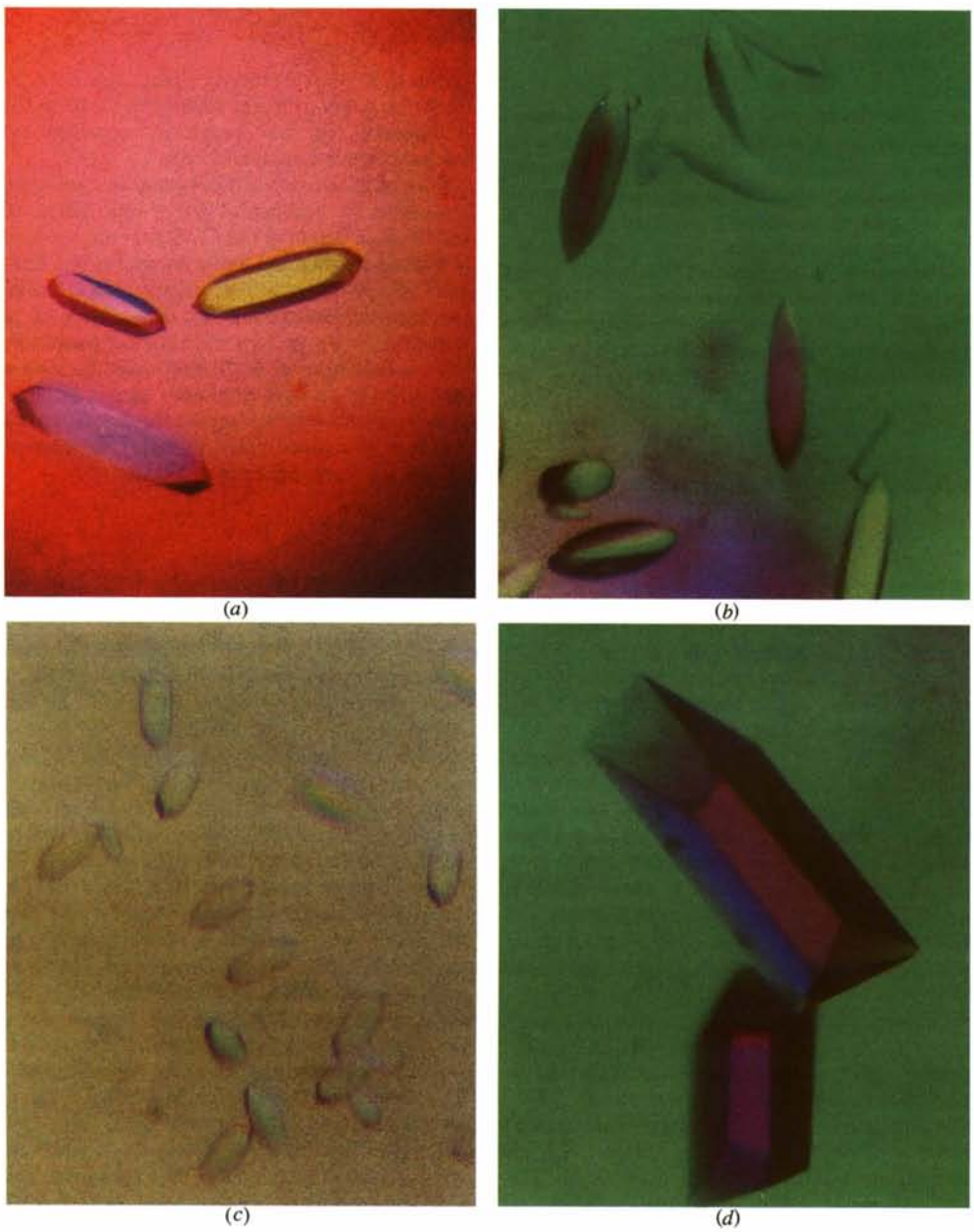

Fig. 1. Photomicrograph of tetragonal and orthohombic CcdB: (*a*) tetragonal crystals grown from ammonium sulfate; (*b*) tetragonal crystals grown from ammonium acetate; (*c*) tetragonal crystals grown from NaCl; (*d*) orthorhombic crystal grown from ammonium sulfate. All photographs are shown on the same scale. The largest crystal in (*d*) is about 0.8 mm long.

Table 1. *Crystals of CcdB*

	Wild type			S74C/G77Q
	Form I	Form II	Form III	Form IV
Space group	$C2$	$P4_22_12$	$P2_12_12_1$	$I222$ or $I2_12_12_1$
Unit cell (Å, °)	a = 74.94 b = 36.24 c = 35.77 β = 115.27	$a = b$ = 104.4 c = 88.9	a = 77.62 b = 93.28 c = 141.44	a = 105.58 b = 105.80 c = 91.90
Resolution (Å)	1.6/1.5†	2.7	2.5	2.5
R_{sym}	0.061/0.056†	0.092	0.070	0.118
Completeness (%)	90.2/84.9†	95.1	93.1	90.2
Multiplicity	6.87/2.33†	2.93	2.97	3.50
Contents of asymm. unit	1 monomer	2 dimers	4 dimers	2 dimers
Solvent contents (%)	35	55	55	55

† After cryocooling.

For the tetragonal and orthorhombic forms, crystallizations were performed at different pH values, ranging from 6.5 to 9.0, using ammonium sulfate, sodium chloride and sodium acetate as precipitants. For the monoclinic form, the pH was chosen between 4.1 and 4.6 using PEG 6000 or PEGMe 5000 as precipitants. For the double S74C/G77Q mutant, a phase diagram was determined using MPD.

Crystallization was also attempted in both agarose and silica gels (Robert *et al.*, 1992; Thiessen, 1994) for tetragonal and monoclinic forms of CcdB. In agarose gels, crystallizations were performed with different concentrations of CcdB ranging from 2.6–5.0 mg ml^{-1}, using 6–12% PEG 6000 and 10–20% PEGMe 5000 as precipitant at pH 4.50 for the monoclinic form. For the tetragonal form, the protein concentration was varied between 6.0 and 12.0 mg ml^{-1} and the concentration of ammonium sulfate between 0.8 and 2.0 *M*. These trials were carried out at both pH 7.5 and pH 8.5. The agarose concentration was varied from 0 to 2% agarose for all conditions tried. Similarly, the silica gel contents were varied from 2.7 to 5.0%.

Crystallization experiments in a microgravity environment of CcdB and its mutants were accepted by ESA for the two missions: USML-2 (1995) and LMS (1996). Hanging-drop (HD) reactors and free-interface diffusion (FID) reactors of the Advanced Protein Crystallization Facility (APCF) were used in these experiments. All experiments were duplicated in identical setups on earth, and in the cases where no crystals appeared during the Space Shuttle mission, the reactors were reactivated on earth after the flight. During the USML-2 mission, one hanging-drop reactor and one FID reactor were allocated for both the wild-type CcdB and for the double mutant S74C/G77Q. During the LMS mission, a single hanging-drop reactor and two FID reactors were also available, but for the wild-type protein only.

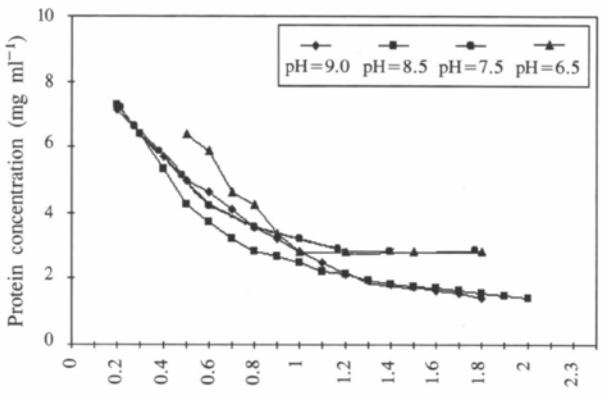

Fig. 2. The solubility of CcdB as a function of pH, ▲ pH 6.5, ● pH 7.5, ■ pH 8.5, ◆ pH 9.0. The experiments were carried out using the hanging-drop technique: 5 µl of protein solution was mixed with 5 µl of bottom solution. The precipitant concentration corresponds to the one in the bottom solution (1.0 ml) at the start of the experiment. Protein concentration was measured after crystal growth ceased. Each experiment was performed in triplicate.

2.4. *Data collection and heavy-atom screening*

Data were collected on an Enraf–Nonius FAST area detector with a rotating-anode source operated at 40 kV and 90 mA. Crystals were mounted in capillaries in the usual way

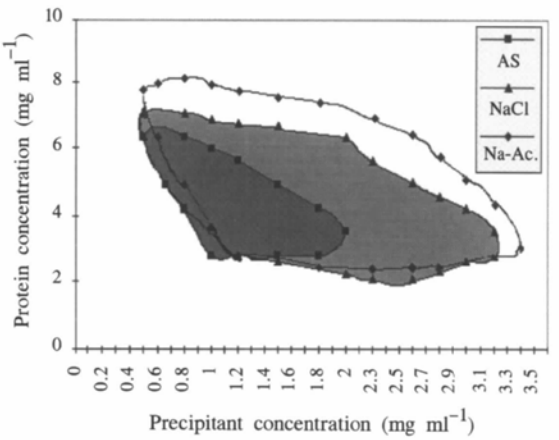

Fig. 3. The crystallization zones of tetragonal CcdB wt in 100 m*M* HEPES pH 7.50 using ammonium sulfate (■), sodium chloride (▲) and sodium acetate (◆) as precipitants. The experiments were performed using the hanging-drop technique: 5 µl of protein solution was mixed with 5 µl of bottom solution. Protein concentrations correspond to the initial concentrations after this initial mixing step before any crystals or precipitate is formed. The precipitant concentration corresponds to the one in the bottom solution (1.0 ml) at the start of the experiment. Each experiment was carried out in triplicate. Crystals appear on the gridpoints inside and on the borders of the shaded areas.

and data were collected at 288 K. In the case of monoclinic CcdB, data were also collected at 100 K. These crystals were first transferred to a solution containing 30%(*w*/*w*) PEG 400 and 70%(*w*/*w*) of a buffer solution consisting of 100 m*M* sodium acetate buffer, pH 4.5, and then shock-frozen in a 100 K nitrogen stream.

Heavy atom-derivatives were screened by adding 1 µl of the corresponding compound (dissolved in the mother liquor of the corresponding crystal form) directly to 10 µl hanging drops containing one or more single crystals of monoclinic CcdB. Soaking times and concentrations were varied from 0.1 m*M* and 1 h to 25 m*M* and 5 d, after which they were mounted in glass capillaries and the data were collected immediately.

3. Results and discussion

3.1. *Tetragonal and orthorhombic crystals*

Four years ago, we reported the crystallization of CcdB in two crystal forms (Steyaert *et al.*, 1993). These were tetragonal

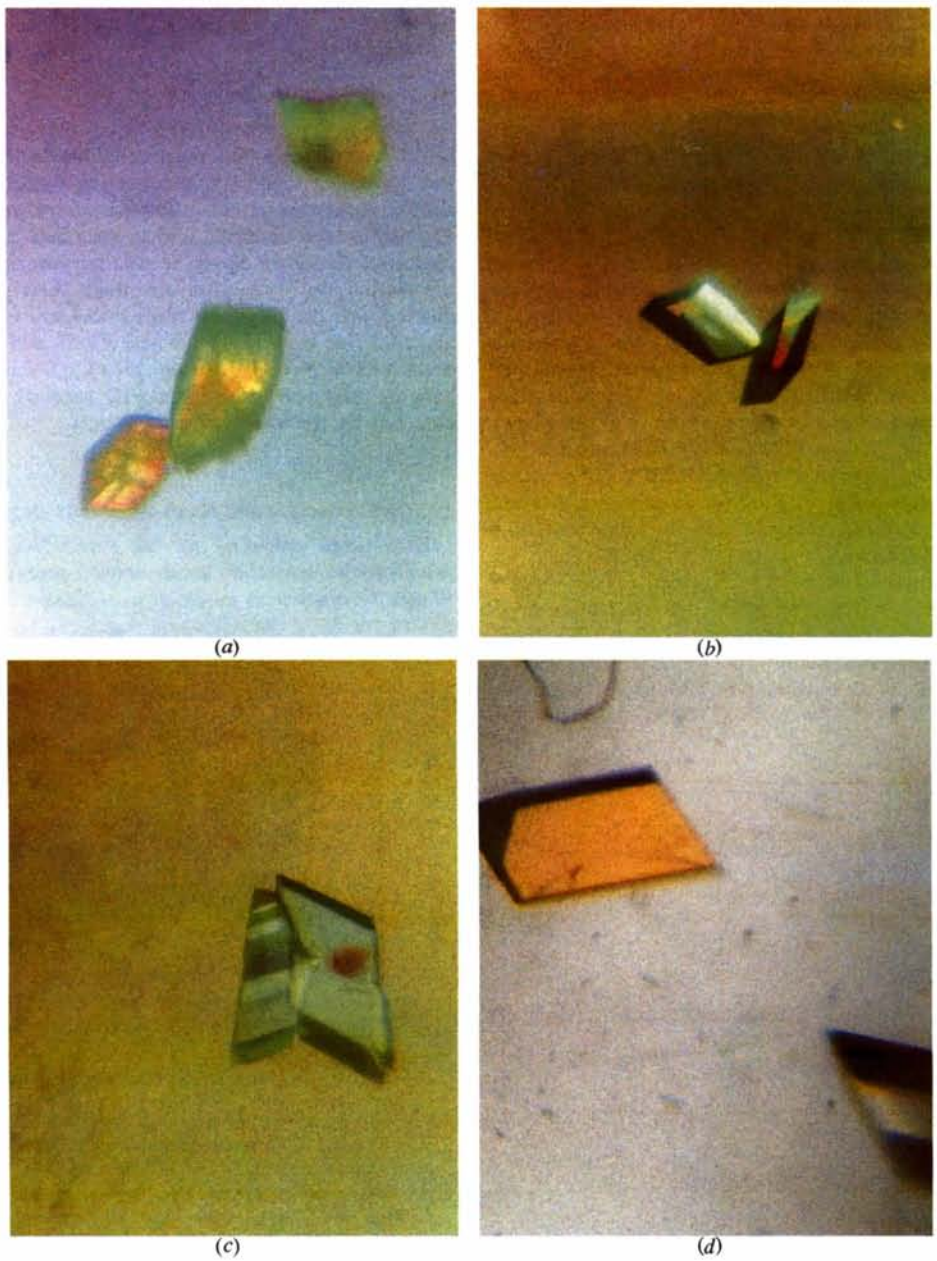

Fig. 4. Monoclinic CcdB crystals; (*a*) spontaneously grown, heavily twinned monoclinic crystals; (*b*) monoclinic crystals grown using microseeding; (*c*) monoclinic crystals grown in agarose gel; (*d*) space-grown monoclinic crystals. All photographs are shown on the same scale. The largest crystal is about 0.3 mm long.

and orthorhombic crystals, the details of which are summarized in Table 1 and their morphologies shown in Fig. 1. The tetragonal and orthorhombic crystals can be grown using ammonium sulfate, sodium chloride and sodium acetate in the pH range 6.5–9.0. The tetragonal crystals grow more easily, while the orthorhombic form occurs more sporadically, often together with tetragonal crystals. Fig. 2 shows the solubility diagram of CcdB protein as a function of ammonium sulfate concentration at different pH values. Fig. 3 shows the crystallization zones of CcdB in 100 m*M* HEPES (pH 7.50) using ammonium sulfate, sodium chloride and sodium acetate as precipitants. The size of the crystallization zone is clearly dependent upon the precipitant type, and the observed diffraction quality for a given precipitant is inversely correlated to the area of the zone where crystals can be grown.

The asymmetric unit of each of these two crystal forms is rather large, and both crystal forms proved to be unusable for heavy-atom screening. In the case of the tetragonal form, a 2.7 Å data set could be collected initially from a crystal grown in ammonium sulfate, but the crystals often showed no significant diffraction at all. This was especially problematic for crystals grown in sodium acetate, although some of them reached dimensions up to 0.4 × 0.5 × 1.5 mm. Also, no suitable heavy-atom derivatives could be found.

The orthorhombic crystals allowed a 2.5 Å native set of data to be collected and consequently, derivative screening was started using these crystals. All prepared potential derivatives were highly non-isomorphous. As apparently all heavy-atom compounds tested showed these same results, regardless of concentration and soaking time, a number of native data sets was collected for comparison. Native data from different crystals turned out to be non-isomorphous to each other, the R_{merge}'s being in the range 30–50%.

3.2. *Monoclinic crystals*

Extensive screening of the crystallization conditions led to a new, monoclinic, low-pH crystal form (Fig. 4). These crystals belong to space group *C*2, with unit-cell parameters a = 74.94, b = 36.24, c = 35.77 Å, β = 115.27°. These crystals grow around pH 4.5 using PEG 6000 or PEGMe 5000 as precipitants. Typically, a drop consisted of 5 µl protein (3 mg ml^{-1} in 100 m*M* MOPS buffer, pH = 7.0) and 5 µl of 10–15% PEG 6000 or PEGMe 5000 in 100 m*M* acetate buffer, pH 4.1–4.5. The monoclinic crystal form contains only a single molecule in the asymmetric unit. Therefore, at low pH, CcdB is at most a dimer, with a molecular twofold axis coinciding with the crystallographic twofold axis of space group *C*2.

Fig. 5 shows the phase diagram of the *C*2 crystal form in 100 m*M* sodium acetate buffer, pH 4.6, and 0.2 *M* ammonium sulfate using PEGMe 5000 as the precipitant. The zone in which crystallization occurs is very narrow and the crystals appear only after precipitation has already formed in the drop. Such a narrow crystallization zone is unusual and makes screening with a wide-grid or sparse-matrix method difficult. Nevertheless, it is this crystal form that forms the key for obtaining the three-dimensional structure of CcdB as it is the only one with which we could prepare useful heavy-atom derivatives. The crystals that grow spontaneously are highly twinned and are not suitable for data collection. To produce single crystals of the *C*2 form, crystallization was performed by using repeated microseeding in both hanging-drop and sitting-drop experiments. The monoclinic CcdB crystals grown in this way turn out to be highly mosaic, and show a large variation in mosaicity from crystal to crystal (0.5–3.0° in unfavourable cases). We were, however, unable to fine-tune the crystallization conditions in order to grow crystals with a lower mosaicity reproducibly, despite extensive efforts, including attempts with gel growth and crystal growth in microgravity conditions (see below). This is in contrast to the results obtained with other proteins using similar techniques (Sica *et*

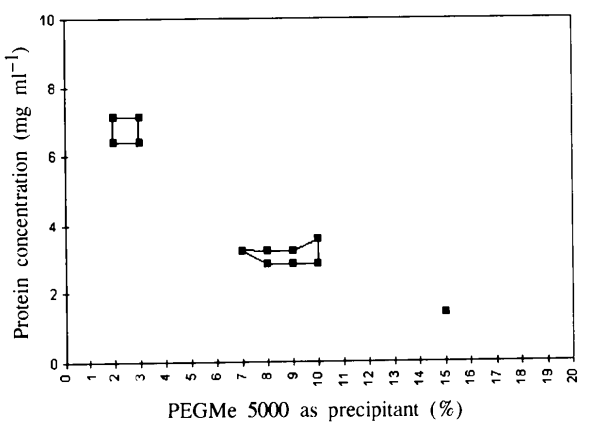

Fig. 5. Crystallization zone of the *C*2 form in 100 sodium acetate buffer, pH 4.6, and 0.2 *M* ammonium sulfate using PEGMe 5000 as precipitant. Crystals appear on the gridpoints encompassed by the shaded area. Experimental procedures as in Fig. 2.

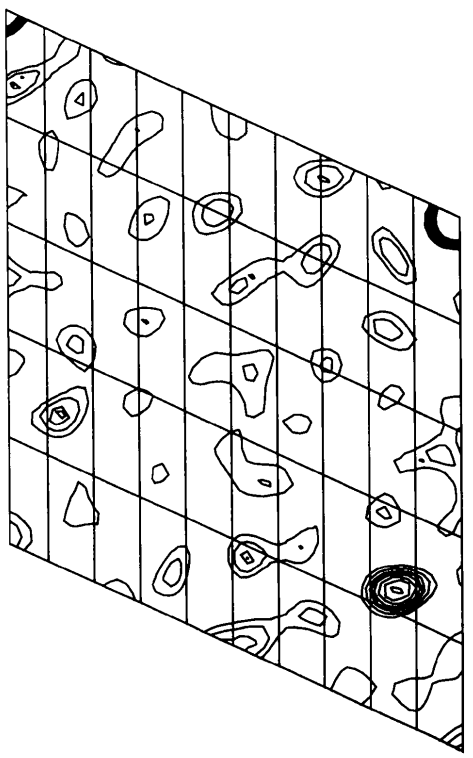

Fig. 6. Harker section v = 0 for the difference Patterson of an Hg derivative of monoclinic CcdB. The map shows contours of 1.0 σ and was calculated at 4.0 Å resolution. One major site is present at coordinates 0.191, y, 0.068.

Table 2. *Overview of the microgravity experiments*

Reactor	Protein drop	Bottom solution/salt chamber	Microgravity	Earth
USLM-2 HD172	50 µl containing 4.5 mg ml^{-1} protein (double mutant S74C/G77Q) in 100 m*M* MOPS, pH 7.0	30 ml containing 30% MPD in 100 m*M* NaAc, pH 4.6	Small amount of precipitation and a few needle-shaped crystals	Larger needle shaped crystals
USLM-2 HD127	30 µl containing 3.7 mg ml^{-1} protein in 100 m*M* MOPS, pH 7.0	50 µl containing 10% PEG 5000 in 100 m*M* NaAc, pH 4.6	Heavy precipitation, a large number of twinned crystals with an average size of 0.3 × 0.2 × 0.2 mm and a few single crystals with average dimensions 0.1 × 0.05 × 0.02 mm	No crystals
LMS HD 154	40 µl containing 4.5 mg ml^{-1} CcdB in 100 m*M* MOPS, pH 7.0	40 µl containing of 10% PEGMe 5000 in 100 m*M* NaAc, pH 4.1	Slight precipitation and a large number of crystals, mostly single	Small, heavily twinned crystals
USLM-2 FID207	115 µl containing 4.5 mg ml^{-1} protein (double mutant S74C/G77Q) in 100 m*M* MOPS, pH 7.0, mixed with 85 ml salt-chamber solution	85 µl containing 2.0 *M* NaCl and 0.2 *M* NaAc in 100 m*M* NaAc, pH 4.6	Heavy precipitation; post-flight re-activation resulted in several needle-shaped crystals	Heavy precipitation; a large number of tiny needle-shaped crystals
USLM-2 FID203B	40 µl containing 7.4 mg ml^{-1} protein in 100 m*M* MOPS, pH 7.0 mixed with 160 ml salt-chamber solution	160 µl containing 10% PEG 5000 in 100 m*M* NaAc, pH 4.6	Slight precipitation; one single crystal (0.05 × 0.02 × 0.02 mm) and several larger twinned crystals	Heavy precipitation; no crystals
LMS FID312B	135 µl containing 4.5 mg ml^{-1} CcdB in 100 m*M* MOPS, pH 7.0, mixed with 65 ml salt-chamber solution	65 µl containing 40% ammonium sulfate in 100 m*M* HEPES, pH 7.5	Small amount of precipitation; no crystals	Heavy precipitation; no crystals
LMS FID305B	80 µl containing 4.5 mg ml^{-1} CcdB in 100 m*M* MOPS, pH 7.0, mixed with 120 ml salt-chamber solution	120 µl containing 10% PEG 5000 in 100 m*M* NaAc, pH 4.1	Small amount of precipitation; no crystals	Heavy precipitation; no crystals

al., 1994; Snell *et al.*, 1995). In fact, high and low mosaicity crystals grow together in the same drop, but there is some tendency for the smaller crystals to be less mosaic. Gel growth resulted in crystals that were essentially similar in size and diffraction quality as those grown in normal hanging- and sitting-drop experiments.

For crystals with high mosaicity, usable diffraction can be observed up to about 3.0 Å, while the better crystals show diffraction up to 1.6 Å at room temperature. This diffraction limit was observed both for crystals grown by microseeding and crystals grown in gel. Data collection on a flash-frozen crystal (refined mosaicity 0.9°) provided usable data up to at least 1.5 Å ($R_{\rm merge}$ in the resolution shell from 1.54 to 1.50 Å was 0.146, with a mean $I/\sigma(I)$ in this shell of 7.2. Screening for heavy-atom derivatives has, until now, resulted in the identification of one single-site derivative. This $Hg(Ac)_2$ derivative was prepared by a 20 h soak in 10 m*M* mercury acetate. The Harker section of the corresponding difference Patterson is shown in Fig. 6, and shows one prominent major site. The structure of CcdB will, therefore, be determined using MIR methods after additional derivatives have been found or, alternatively, using multiwavelength anomalous diffraction (MAD) on the single-site $Hg(Ac)_2$ derivative.

3.3. *Crystallization in a microgravity environment*

Crystal growth in microgravity conditions was used as a possible solution to overcome the problem of twinning and high mosaicities. The experimental conditions used as well as the outcome of these experiments are summarized in Table 2. The number of experiments that could be performed during the two Space Shuttle missions was limited, and the interpretation is complicated by the failure to grow crystals in most of the control experiments on earth. Nevertheless, the fact that crystals could be grown in several reactors during the Space Shuttle missions, while no crystals appeared in the control experiments on earth does suggest that the lack of convection and sedimentation has a beneficial effect on protein-crystal growth. In the one experiment in which crystals were produced both in space and on earth, we did observe a significant decrease of the number of twinned crystals, but no pronounced improvement of the mosaicity was evident.

3.4. *Crystallization of cysteine mutants*

To look for suitable heavy-metal derivatives, we decided to make the following four specific serine-to-cysteine mutants, Ser70Cys, Ser74Cys, Ser84Cys and the double mutant Ser74Cys/Gly77Gln. These mutants were designed for the production of Hg derivatives in the MIR work and some of them were shown to act as super-killers (Bahassi *et al.*, 1998). No crystals were obtained for the two mutants Ser74Cys and Ser84Cys. The mutant Ser70Cys crystallized in ammonium sulfate as very thin plates that do not give single-crystal diffraction patterns. The double mutant Ser70Cys/Gly77Gln was initially crystallized using MPD as precipitant. The crystals thus formed were thin needles that diffract to at best 7 Å and do not withstand soaking with mercury salts. In the later experiments, well diffracting crystals were formed in the same conditions as those in which the wild-type protein produces the tetragonal form. These crystals are, however, not isomorphous with the those of the wild-type protein. They belong to space

group $I222$ (or $I2_12_12_1$) with unit cell $a = 105.58$, $b = 105.80$, $c = 91.90$ Å and diffract to 2.5 Å resolution (Table 1). Although a and b are almost identical and the unit-cell constants are very similar to the tetragonal form of the wild-type protein, the crystals are not tetragonal. Nevertheless, both crystal forms are probably related, as the tetragonal form of the wild-type protein contains a 17σ non-origin peak in its Patterson, suggesting pseudocentering (data not shown).

This work was supported by the Vlaams Interuniversitair Instituut voor Biotechnologie. We thank ESA for the IML-2/APCF grant. We thank Maria Vandervcken, James Leten and Li Yan for excellent technical assistance. We are also grateful to Dr R. Giegé and Dr Joseph Ng (CNRS, Strasbourg, France) for guiding the experiment in gels. R. Loris is a research associate of the FWO.

References

Bahassi, E. M., Jaloveckas, D. R. & Couturier, M. (1998). In preparation.

Bailone, A., Sommer, S. & Devoret, R. (1985) *Proc. Natl Acad. Sci. USA*, **82**, 5973–5977.

Bernard, P. & Couturier, M. (1992) *J. Mol. Biol.* **226**, 735–745.

Bernard, P., Kézdy, K., Van Melderen, L., Steyaert, J., Wyns, L., Pato, M., Higgins P. & Couturier, M. (1993). *J. Mol. Biol.* **234**, 534–541.

Bex, F., Karoui, H., Rokeach, L., Drèze, P., Garcia, L. & Couturier, M. (1983). *EMBO J.* **2**, 1853–1861.

De Feyter, R., Wallace, C. & Lane, D. (1989). *Mol. Gen. Genet.* **218**, 481–486.

Jaffé, A., Ogura, T. & Hiraga, S. (1985) *J. Bacteriol.* **163**, 841–849.

Karoui, H., Bex, F., Drèze, P. & Couturier, M. (1983). *EMBO J.* **2**, 1863–1968.

Miki, T., Chang, Z.-T. & Horiuchi, T. (1984). *J. Mol. Biol.* **174**, 627–646.

Miki, T., Yashioka, K. & Horiuchi, T. (1984). *J. Mol. Biol.* **174**, 605–626.

Robert, M. C., Provost, K. & Lefaucheux, F. (1992). In *Crystallization of Nucleic Acids and Proteins. A Practical Approach*, edited by A. Ducruix & R. Giegé. Oxford University Press.

Sica, F., Demasi, D., Mazzarella, A., Zagari, A. & Capasso, S. (1994). *Acta Cryst.* D**50**, 508–511.

Snell, E. H., Weisgerber, S., Helliwell, J. R., Weckert, E., Hölzer, K. & Schroer, K. (1995). *Acta Cryst.* D**51**, 1099–1102.

Steyaert, J., Van Melderen, L., Bernard, P., Dao-Thi, M.-H., Loris, R., Wyns, L. & Couturier, M. (1993). *J. Mol. Biol.* **231**, 513–515.

Tam, J. E. & Kline, B. C. (1989*a*). *Mol. Gen. Genet.* **219**, 26–32.

Tam, J. E. & Kline, B. C. (1989*b*). *J. Bacteriol.* **171**, 2353–2360.

Thiessen, K. J. (1994). *Acta Cryst.* D**50**, 491–495.

Van Melderen, L., Bernard, P. & Couturier, M. (1994). *Mol. Microbiol.* **11**, 1151–1157.

Van Melderen, L., Dao-Thi, M.-H., Lecchi, P., Gottesman, S., Couturier, M. & Maurizi, M. R. (1996). *J. Biol. Chem.* **271**, 27730–27738.